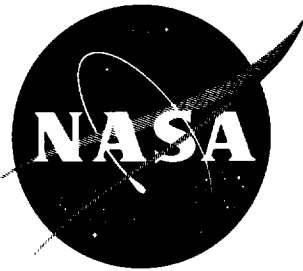


N63-18469

NASA TN D-1938

NASA TN D-1938



TECHNICAL NOTE

D-1938

A TRAJECTORY ANALYSIS OF A VARIABLE-DRAG PAYLOAD
EJECTED FROM A VEHICLE IN A LOW EARTH ORBIT

By Richard Reid and David B. Middleton

Langley Research Center
Langley Station, Hampton, Va.

NATIONAL AERONAUTICS AND SPACE ADMINISTRATION
WASHINGTON

July 1963

<p>NASA TN D-1938</p> <p>National Aeronautics and Space Administration.</p> <p>A TRAJECTORY ANALYSIS OF A VARIABLE-DRAG PAYLOAD EJECTED FROM A VEHICLE IN A LOW EARTH ORBIT. Richard Reid and David B. Middleton. July 1963. 28p. OTS price, \$0.75. (NASA TECHNICAL NOTE D-1938)</p> <p>A limited analytical study has been made of the trajectories of a small variable-drag payload ejected at low velocity from a vehicle in a low earth orbit. Useful trajectories are determined for dispatching the payload to desired regions for space experimentation. Alteration of the basic trajectories is accomplished by means of the variable-drag feature. The drag effects are studied in terms of changing the ballistic number of the payload at predetermined points along the basic trajectories.</p>	<p>I. Reid, Richard</p> <p>II. Middleton, David B.</p> <p>III. NASA TN D-1938</p>	<p>NASA</p>
<p>NASA TN D-1938</p> <p>National Aeronautics and Space Administration.</p> <p>A TRAJECTORY ANALYSIS OF A VARIABLE-DRAG PAYLOAD EJECTED FROM A VEHICLE IN A LOW EARTH ORBIT. Richard Reid and David B. Middleton. July 1963. 28p. OTS price, \$0.75. (NASA TECHNICAL NOTE D-1938)</p> <p>A limited analytical study has been made of the trajectories of a small variable-drag payload ejected at low velocity from a vehicle in a low earth orbit. Useful trajectories are determined for dispatching the payload to desired regions for space experimentation. Alteration of the basic trajectories is accomplished by means of the variable-drag feature. The drag effects are studied in terms of changing the ballistic number of the payload at predetermined points along the basic trajectories.</p>	<p>I. Reid, Richard</p> <p>II. Middleton, David B.</p> <p>III. NASA TN D-1938</p>	<p>NASA</p>
<p>NASA TN D-1938</p> <p>National Aeronautics and Space Administration.</p> <p>A TRAJECTORY ANALYSIS OF A VARIABLE-DRAG PAYLOAD EJECTED FROM A VEHICLE IN A LOW EARTH ORBIT. Richard Reid and David B. Middleton. July 1963. 28p. OTS price, \$0.75. (NASA TECHNICAL NOTE D-1938)</p> <p>A limited analytical study has been made of the trajectories of a small variable-drag payload ejected at low velocity from a vehicle in a low earth orbit. Useful trajectories are determined for dispatching the payload to desired regions for space experimentation. Alteration of the basic trajectories is accomplished by means of the variable-drag feature. The drag effects are studied in terms of changing the ballistic number of the payload at predetermined points along the basic trajectories.</p>	<p>I. Reid, Richard</p> <p>II. Middleton, David B.</p> <p>III. NASA TN D-1938</p>	<p>NASA</p>

NATIONAL AERONAUTICS AND SPACE ADMINISTRATION

TECHNICAL NOTE D-1938

A TRAJECTORY ANALYSIS OF A VARIABLE-DRAG PAYLOAD

EJECTED FROM A VEHICLE IN A LOW EARTH ORBIT

By Richard Reid and David B. Middleton

SUMMARY

A limited analytical study has been made of the trajectories of a small variable-drag payload ejected at low velocity from a vehicle in a low earth orbit. Useful trajectories are determined for dispatching the payload to desired regions for space experimentation. Alteration of the basic trajectories is accomplished by means of the variable-drag feature. The drag effects are studied in terms of changing the ballistic number of the payload at predetermined points along the basic trajectories.

The results of the study are presented as plots of distance and velocity relative to the orbiting vehicle. Particular emphasis is given to the determination of parameter combinations which lead to conditions favorable for using the payload as a target for rendezvous practice. The combinations adjudged most favorable are: (1) low ejection velocities, (2) ejection in the direction of the center of the earth, (3) ballistic-number change (reduction) of about two orders of magnitude, and (4) ballistic-number change near the perigee of the payload orbit. The results of ballistic-number changes near the apogee of the payload orbit are also included.

The results of this study indicate that the scheme of ejecting a variable-drag payload from an orbiting vehicle can be developed into a useful method of space experimentation. The trajectories obtainable are limited only by the ejection velocity and weight-area ratio of the payload. Payload trajectories can be predetermined, within the accuracies of the parameters, for particular experiments by using the approach of this study.

INTRODUCTION

In future space flights, many experiments will be carried out to study the earth's environment and to optimize flight maneuvers such as rendezvous and docking. A suggested method to aid in preliminary studies and the accumulation of data is the technique of carrying payloads into a low earth orbit aboard a manned vehicle and later ejecting them for use in various experiments.

A limited analytical study of the trajectories of ejected payloads has been made and the results are reported herein. The analysis used is similar to that of reference 1. Reference 1 is a trajectory study concerned with the terminal phase of rendezvous from an earth launch and the initial phase of the ejection or return-to-earth trajectory. However, in the present study ejection trajectories were modified by the inclusion of atmospheric effects and variable-drag capabilities. The variable drag is studied in terms of reducing the ballistic number of the payload at preset times after ejection by releasing and inflating a tethered balloon.

After some preliminary runs and an examination of the data, it was decided to confine the main portion of the study to cases in which the payload remained primarily ahead of the orbiting vehicle. Particular emphasis was given to the establishment of cases in which the ballistic number was changed after the payload reached a distance of approximately 1 mile ahead of the vehicle and the payload then retained a low rate of separation for 15 minutes or longer. These cases were deemed most suitable for using the payload as a target for rendezvous practice. Also of interest were trajectories in which the payload would make a relatively fast pass-by of the vehicle and thus create a worthwhile tracking task.

The results are presented as plots of position and velocity of the payload relative to the orbiting vehicle. The trajectories were developed from digital-computer solutions of the equations of motion.

SYMBOLS

The English system of units is used in this study. In case conversion to metric units is desired, the following relationships apply:

$$1 \text{ international foot} = 0.3048 \text{ meter}$$

$$1 \text{ international statute mile} = 5,280 \text{ feet} = 1,609.344 \text{ meters}$$

A cross-sectional area

C_D drag coefficient

D drag force, $C_D A \rho V^2 / 2$

E_k kinetic energy

E_p potential energy

g acceleration due to gravity

\bar{h} altitude of vehicle with respect to the earth's surface

\bar{i}, \bar{j}	unit vectors in the direction of the X- and Y-axis, respectively
L	Lagrangian, $E_k - E_p$
m	mass of ejected payload
N_B	ballistic number, $W/C_D A$
\bar{R}	range vector or separation distance between vehicle and ejected payload
\bar{r}	radial distance measured from the center of the earth
t	time
$\overline{\Delta V}$	relative velocity vector of ejected payload with respect to the vehicle
\bar{V}	velocity vector of the vehicle with respect to the center of the earth
W	weight
X, Y	Cartesian axes moving with the vehicle and oriented so that the positive Y-axis is always pointed radially away from the center of the earth and the negative X-axis is in the direction of vehicle motion
x, y	coordinates along X- and Y-axis, respectively
\dot{x}, \dot{y}	components of velocity in the X,Y axis system
\ddot{x}, \ddot{y}	components of acceleration in the X,Y axis system
β	constant used in exponential approximation of atmospheric density
ρ	weight density of earth's atmosphere
$\bar{\Omega}$	angular velocity of ejected payload with respect to the X,Y axis system
$\bar{\omega}$	angular velocity of X,Y axis system

Subscripts:

e	earth
m	ejected payload
o	value at instant of ejection
s	vehicle
x	measure of variable in X-direction
y	measure of variable in Y-direction

- 1 prior to balloon inflation
- 2 after balloon inflation

GENERAL CONSIDERATIONS AND PROCEDURES

The angular velocity ω of a satellite about the center of the earth is constant for a circular orbit. A payload ejected from a satellite will have a linear velocity with respect to the satellite at each instant of time. A component of this velocity pointed radially away from the center of the earth will result in a movement of the payload outward and a decrease in ω due to the conservation of angular momentum. With decreasing ω , the payload will move behind the satellite. Similarly, a component of velocity in the direction opposite to the satellite's motion will result in a lower value of ω for the payload and it will move behind and then below the satellite. As it moves below, it will acquire an increased ω and it will then move ahead of the satellite.

Alteration of the path and velocity pattern can be accomplished by changing the ballistic number of the payload. From an initial value of 45, the ballistic number was changed arbitrarily to 4.0, 0.4, and 0.04 in the preliminary calculations. The value of 0.4 was selected for the main study because it seemed feasible from the hardware standpoint and because it was sufficiently low for the drag effects of the payload to be utilized and yet high enough to preclude rapid changes in the payload motion. Thus, a ballistic-number change from 45 to 0.4 at preset times along the trajectory became a standard feature of the present study, in which the following assumptions were made:

1. The ballistic number of the orbiting vehicle is 45, and it has carried into orbit a small rigid payload with an equal ballistic number.
2. The payload will be separated from the vehicle with a low impulsive relative velocity, and the payload contains a folded balloon with the capability of inflation at any desired time after ejection (to reduce the ballistic number of the payload).
3. The vehicle is in a 150-mile circular orbit around a spherical earth at the time of ejection of the payload.
4. The trajectories of the ejected payload are confined to the plane of the vehicle's orbit.
5. All motions are measured with respect to a rotating set of Cartesian coordinates fixed at the center of mass of the vehicle. As shown in figure 1, the motion of the vehicle is in the negative X-direction with the positive Y-axis always pointed radially away from the center of the earth.
6. The time intervals of consideration are less than or equal to one period of the vehicle's orbit.

A basic trajectory is herein defined as the path the ejected payload will follow if no balloon is deployed; for a selected ejection velocity this path is dependent upon the ejection angle. The case of an ejection velocity of 10 fps is shown in figure 2 for combinations of velocity components representing trajectories over the full range of ejection angles. Elapsed time from ejection is indicated by tick marks at 5-minute intervals and each trajectory is terminated after 25 minutes. Thus, any basic trajectory is attainable within the capability of the ejection velocity, but this study was limited to ejection radially toward the center of the earth.

When alterations in the basic path and relative velocity are desired, the folded balloon is released and inflated, thus significantly changing the ballistic number of the payload.

EQUATIONS OF MOTION

The equations are essentially those derived in reference 2 and also used in reference 1. Modification of the equations was necessary to introduce atmospheric-drag effects.

The atmospheric-drag effects were included as a function of atmospheric density, velocity, and ballistic number. The method of Lagrange was employed in deriving the equations of motion based on the kinetic and potential energy of the ejected payload at any instant. The following equations were used in the investigation:

$$\ddot{x} - 2\omega\dot{y} + x\left(\frac{g_e r_e^2}{r_m^3} - \omega^2\right) = \frac{1}{2N_B} \rho_0 e^{\beta y} [\dot{x} - (y + r_s)\omega]^2$$

$$\ddot{y} + 2\omega\dot{x} + (y + r_s)\left(\frac{g_e r_e^2}{r_m^3} - \omega^2\right) = \frac{1}{2N_B} \rho_0 e^{\beta y} (y + x\omega)^2$$

Derivation of the equations, along with a brief discussion of atmospheric drag, is included in the appendix.

RESULTS AND DISCUSSION

Most of this report is concerned with the results of ejecting a payload radially toward the center of the earth at 2 fps and 10 fps. Since it is assumed

that the velocity imparted to the payload is due to impulsive thrust, initially the payload has zero relative velocity in the X-direction and either -2 or -10 fps in the Y-direction for the cases considered. With such small initial velocities there is very little shift in the apsidal line, and the payload follows an elliptical path always in front of the vehicle. These basic trajectories relative to the vehicle are shown in figure 3(a) for one orbit of the earth. Tick marks are placed at 5-minute intervals on the trajectory. When no balloon is deployed, the payload returns essentially to the point of ejection after one orbital period. Figure 3(b) is a plot of the relative velocity distribution over these basic trajectories. The tick marks here (and on all following figures) also represent 5-minute intervals from ejection. The total relative velocity of the payload with respect to the vehicle at any time is the velocity vector from the origin of the graph to the point on the velocity curve corresponding to the time.

At times when the relative velocity of the payload is primarily in the negative X-direction, a sudden reduction in the ballistic number of the payload results in a reduction in the x velocity component with little immediate change in the y component. For example, in figure 4 the ballistic number is changed near the perigee of the payload orbit. Here, the payload possesses maximum supercircular velocity (maximum kinetic energy) and the longest time is required to null the x component of the relative velocity. As the payload slows to sub-circular velocity it turns toward the earth, and then it increases in relative velocity as it reenters the denser atmosphere. In figure 4, the payload is ejected at 2 fps toward the center of the earth and the ballistic number of the payload is changed from 45 to 0.4 at 20, 22.5, and 25 minutes after ejection, respectively. Figure 4(a) shows the motion of the payload relative to the vehicle. After balloon deployment at 20, 22.5, and 25 minutes, the trajectories are plotted for an additional 14, 16, and 15 minutes, respectively. Figure 4(b) illustrates the changes in \dot{x} and \dot{y} due to the decrease in ballistic number. That is, by comparing figure 4(a), where the ballistic number is changed, with the corresponding (same initial velocity) case of figure 3(a), where the ballistic number is not changed, the effects of decreasing this number can be easily seen. Similar data are prepared (figs. 5(a) and 5(b)) for the case of an ejection velocity of 10 fps and the same ballistic-number change at the same times after ejection.

At the highest altitude of the payload (apogee of payload orbit), the payload possesses its minimum kinetic energy. When the ballistic number is reduced at this point, the effect is to start immediate decay of the orbit (since the payload velocity is already subcircular). This further slowing down below circular velocity causes the payload to cross the vehicle orbit behind the vehicle; it then increases in velocity and passes ahead of and underneath the vehicle. Figures 6(a) and 6(b) illustrate the case of ejection at 2 fps toward the center of the earth, with balloon deployment at 65, 67.5, and 70 minutes. Figure 6(a) gives the separation distance of the payload with respect to the vehicle and figure 6(b) gives the velocity distribution. Figures 7(a) and 7(b) show similar results for a payload ejection velocity of 10 fps.

To determine the trajectory alterations caused by different reductions in ballistic number at perigee, the case of figure 5 was also investigated for ballistic-number changes to 4.0 and 0.04. A comparison of the trajectories is

presented in figure 8. In view of the rendezvous considerations, the unsuitability of the value 0.04 is apparent from both figures 8(a) and 8(b). The value 0.4 rather than 4.0 was used in this study because the value 0.4 resulted in less change in \dot{y} while reducing \dot{x} .

In cases of ballistic-number reduction near apogee (figs. 6 and 7), the change to 0.4 produces a trajectory in which the payload makes a faster pass-by of the vehicle than with the change to 4.0, and thus provides a more difficult tracking task for the vehicle.

Many combinations of ejection velocity, ejection angle, and ballistic-number change were investigated, but only the trajectories which seem most suitable for the experiments considered are reported. The results indicate that numerous combinations of these parameters are practical for use in designing a variety of space experiments. It is beyond the scope of this paper to discuss or evaluate particular experiments, but the data presented are slanted toward planning such things as a practice rendezvous program (balloon deployment near perigee), vehicle tracking and maneuvering capability (balloon deployment near apogee), or visual acuity tests (balloon deployment anywhere along basic trajectory).

CONCLUDING REMARKS

The results of this analytical study lead to the conclusion that the technique of ejecting a variable-drag payload can be developed into a useful method of space experimentation. Within the accuracies of the parameters, the trajectories of payloads can be predetermined for particular experiments by using the approach of this study. Perhaps the most significant aspect of the ejection concept is that it lends itself readily to multiple launchings from a single orbiting vehicle and thus allows a diversity of experiments to be conducted during a single mission.

The overall effects of variation of ejection velocity, ejection angle, and time of ballistic-number change near the extremes (perigee and apogee) of the payload orbit are shown in the figures. The trajectories which have been developed illustrate the following:

1. That ejection of the payload radially toward the center of the earth at low velocity and a subsequent reduction of its ballistic number from 45 to 0.4 near the perigee of the payload orbit results in the most favorable conditions for rendezvous practice with the payload as a target

2. That ballistic-number change near the apogee of the payload orbit results in a high relative velocity of the payload as it passes by the vehicle and thus sets up a useful tracking task for the vehicle

From the results of this study the character of trajectories altered by ballistic-number change at intermediate points can be deduced, or this study can

be readily extended to the intermediate points of interest, since the equations and analysis are relatively simple.

Langley Research Center,
National Aeronautics and Space Administration,
Langley Station, Hampton, Va., May 8, 1963.

APPENDIX

EQUATIONS OF MOTION IN A ROTATING AXIS SYSTEM

The equations of motion of an ejected payload are derived with respect to rotating Cartesian coordinates fixed at the center of mass of a vehicle in circular orbit. The method of Lagrange is used in the derivation, which is based on the kinetic and potential energy of the payload at any instant. The positions of the vehicle and payload, respectively, are shown in figure 1 to be

$$\bar{r}_s = \bar{r}_e + \bar{h} \quad (A1)$$

$$\bar{r}_m = \bar{r}_s + \bar{R} \quad (A2)$$

where \bar{h} is the extension of \bar{r}_e to the vehicle orbit. The absolute velocity of the payload is given by

$$\bar{V} = \bar{V}_s + \bar{\Delta V} = \frac{d}{dt}(\bar{r}_m) = \frac{d}{dt}(\bar{r}_s) + \frac{d}{dt}(\bar{R}) + (\bar{\Omega} \times \bar{R}) \quad (A3)$$

The vectors in equation (A3) have the following components:

$$\bar{r}_m = (x, y + r_s)$$

$$\bar{R} = (x, y)$$

$$\frac{d}{dt}(\bar{R}) = (\dot{x}, \dot{y})$$

$$\bar{\Omega} \times \bar{R} = (-y\omega, x\omega)$$

$$\frac{d}{dt}(\bar{r}_s) = (-r_s\omega, 0)$$

The absolute velocity of the payload may thus be written in terms of the vehicle coordinates and the constants r_s and ω as

$$\bar{V} = \bar{i}[\dot{x} - (y + r_s)\omega] + \bar{j}(\dot{y} + x\omega) \quad (A4)$$

The kinetic energy of the payload is then

$$\begin{aligned}
E_k &= \frac{m}{2} (\vec{v} \cdot \vec{v}) \\
&= \frac{m}{2} \left\{ \dot{x}^2 + \dot{y}^2 + \omega^2 \left[x^2 + (y + r_s)^2 \right] + 2\omega \left[x\dot{y} - \dot{x}(y + r_s) \right] \right\}
\end{aligned} \tag{A5}$$

The potential energy of the payload is given by

$$E_p = -mgr_m = - \frac{mg_e r_e^2}{r_m} = - \frac{mg_e r_e^2}{\sqrt{x^2 + (y + r_s)^2}} \tag{A6}$$

The Lagrangian can be formed as

$$L = E_k - E_p \tag{A7}$$

and performing the Lagrangian operation

$$\frac{d}{dt} \left(\frac{\partial L}{\partial \dot{x}} \right) - \frac{\partial L}{\partial x} = D_x \tag{A8}$$

yields

$$- \frac{\partial E_k}{\partial x} = m(-\omega^2 x - \omega \dot{y})$$

$$\frac{\partial E_k}{\partial \dot{x}} = m \left[\dot{x} - \omega(y + r_s) \right]$$

$$\frac{\partial E_p}{\partial \dot{x}} = \frac{d}{dt} \left(\frac{\partial E_p}{\partial \dot{x}} \right) = 0$$

$$\frac{\partial E_p}{\partial x} = m \frac{x g_e r_e^2}{r_m^3}$$

$$\frac{d}{dt} \left(\frac{\partial E_k}{\partial \dot{x}} \right) = m(\ddot{x} - \omega \dot{y})$$

Thus the equation giving the relative motion in the X-direction (including drag) is

$$D_X = m \left[\ddot{x} - 2\omega \dot{y} + x \left(\frac{g_e r_e^2}{r_m^3} - \omega^2 \right) \right] \quad (A9)$$

where D_X is the drag as a function of ballistic number, density, and velocity. By similar operation the equation for motion in the Y-direction is found to be

$$D_Y = m \left[\ddot{y} + 2\omega \dot{x} + (y + r_s) \left(\frac{g_e r_e^2}{r_m^3} - \omega^2 \right) \right] \quad (A10)$$

and the equation describing the relative position of the payload is, from equation (A2),

$$r_m = \sqrt{x^2 + (y + r_s)^2} \quad (A11)$$

To determine D_X and D_Y , a density equation was written. Density values for the range of altitudes to be considered were taken from reference 3 and plotted in figure 9. The equation for density written from this curve is

$$\rho = \rho_0 e^{\beta y} \quad (A12)$$

Since weight densities were used, the values of D_X/m and D_Y/m are

$$\left. \begin{aligned} \frac{D_X}{m} &= \frac{1}{2} \frac{C_{DA}}{W} \rho V_x^2 \\ \frac{D_Y}{m} &= \frac{1}{2} \frac{C_{DA}}{W} \rho V_y^2 \end{aligned} \right\} \quad (A13)$$

Substituting $N_B = \frac{W}{C_{DA}}$ and equations (A12) and (A4) into equations (A13) gives the equations of motion used in this report:

$$\ddot{x} - 2\omega\dot{y} + x\left(\frac{g_e r_e^2}{r_m^3} - \omega^2\right) = \frac{1}{2N_B} \rho_o e^{\beta y} [\dot{x} - (y + r_s)\omega]^2$$

$$\ddot{y} + 2\omega\dot{x} + (y + r_s)\left(\frac{g_e r_e^2}{r_m^3} - \omega^2\right) = \frac{1}{2N_B} \rho_o e^{\beta y} (y + x\omega)^2$$

REFERENCES

1. Eggleston, John M., and Beck, Harold D.: A Study of the Positions and Velocities of a Space Station and a Ferry Vehicle During Rendezvous and Return. NASA TR R-87, 1961.
2. Clohessy, W. H., and Wiltshire, R. S.: Terminal Guidance System for Satellite Rendezvous. Jour. Aerospace Sci., vol. 27, no. 9, Sept. 1960, pp. 653-658, 674.
3. Anon.: U.S. Standard Atmosphere, 1962. NASA, U.S. Air Force, and U.S. Weather Bureau, Dec. 1962.

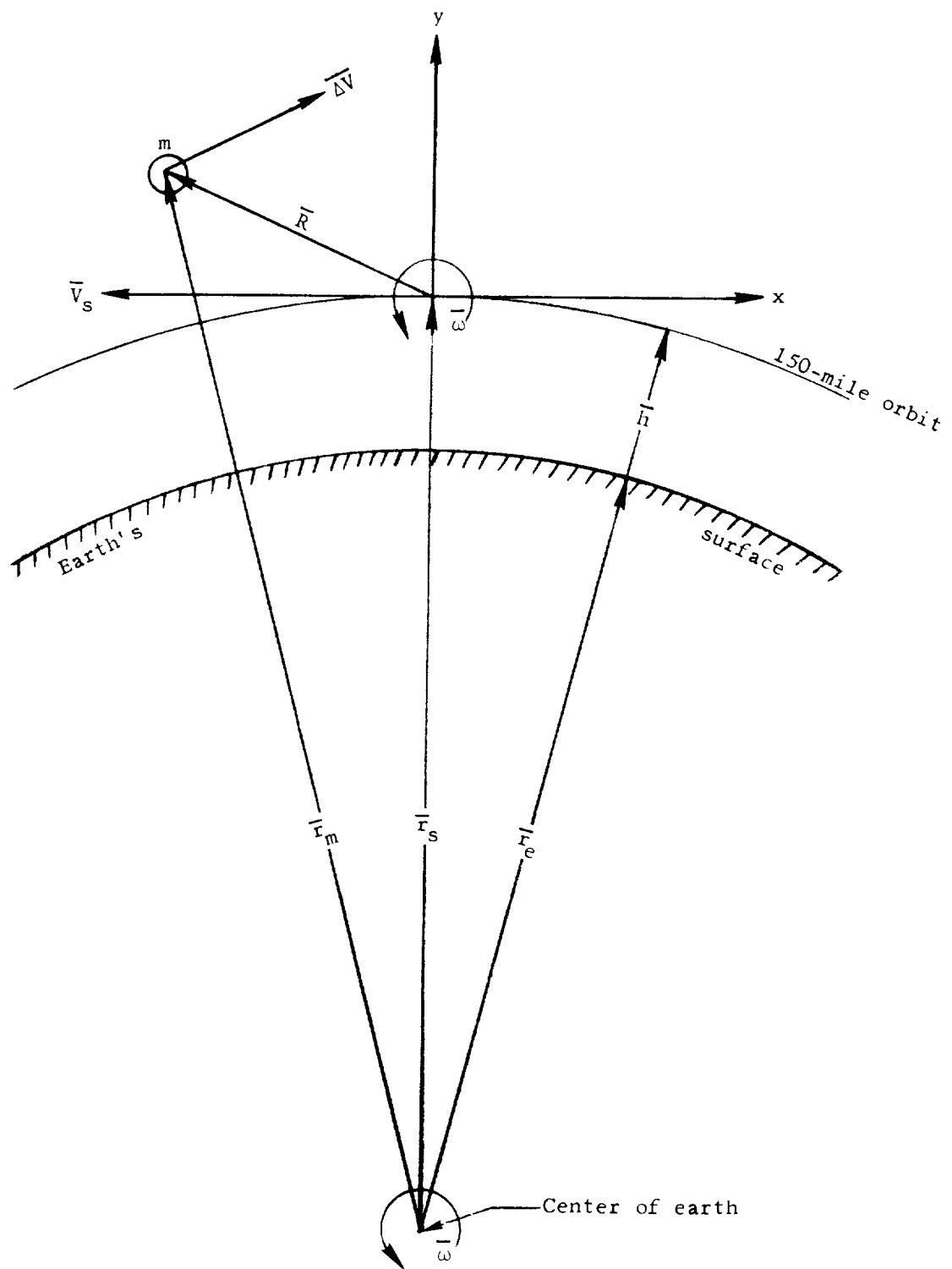
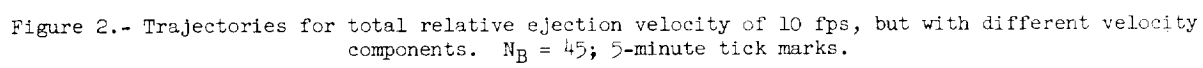
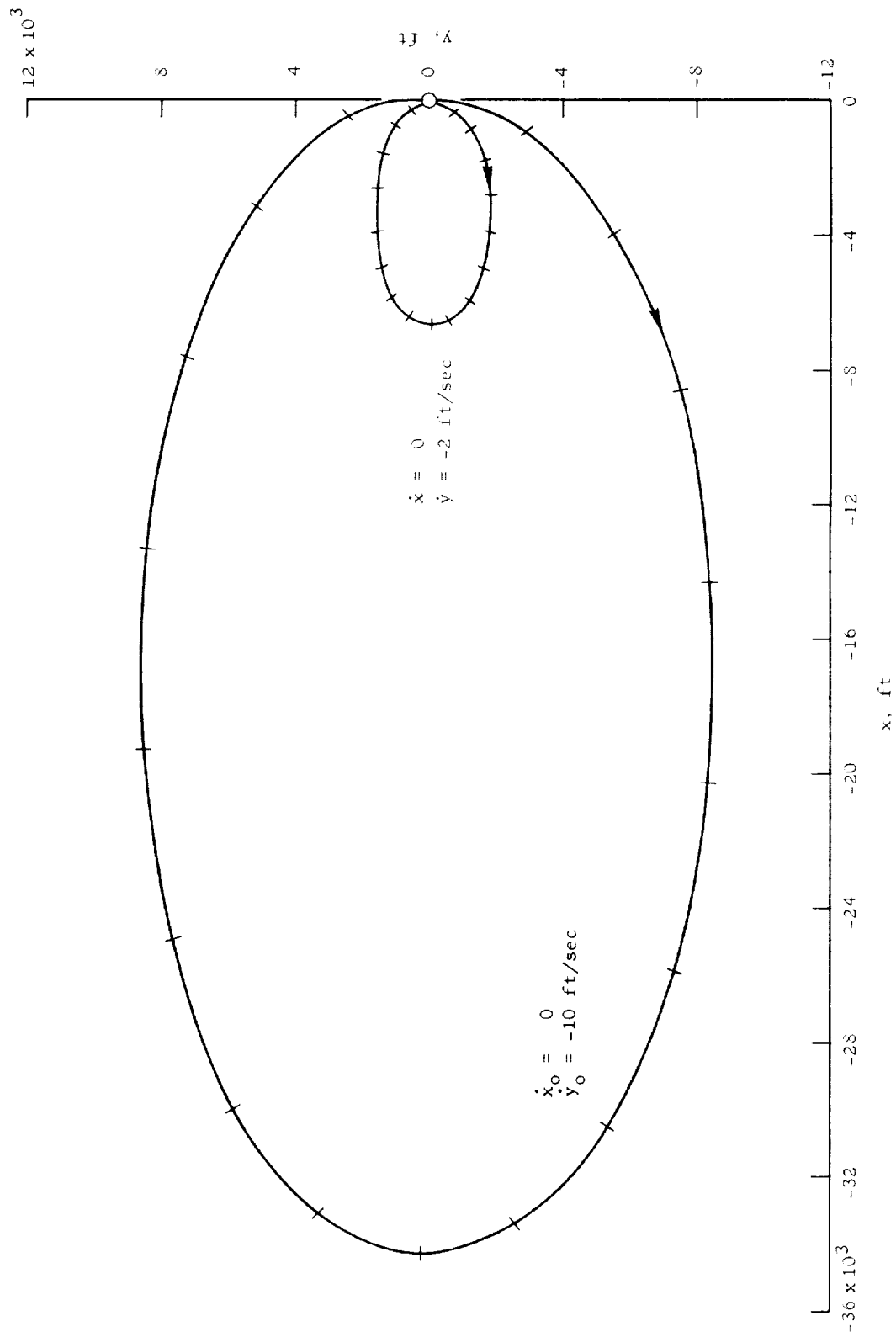


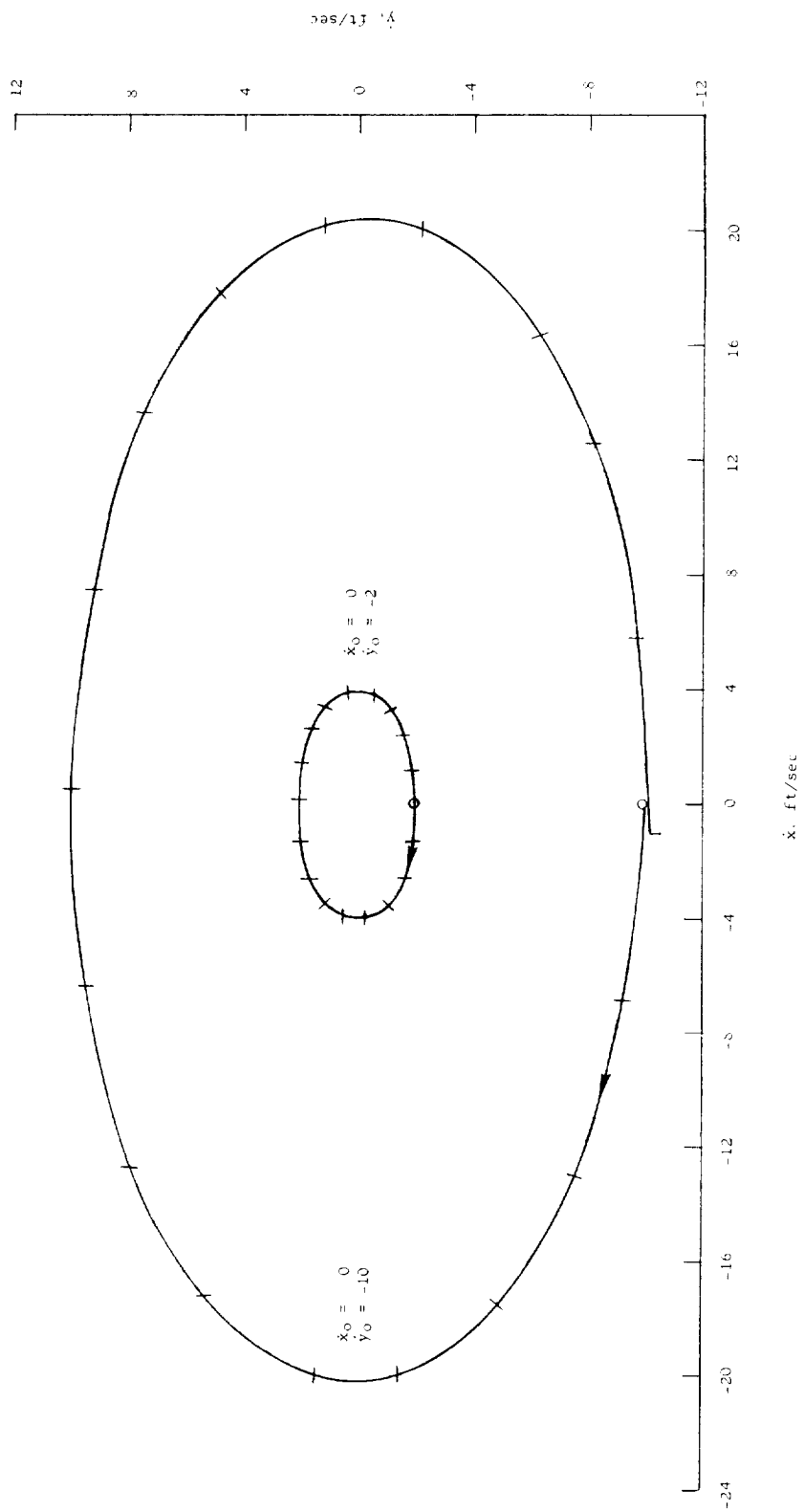
Figure 1.- Geometric relations between orbiting vehicle and ejected payload.





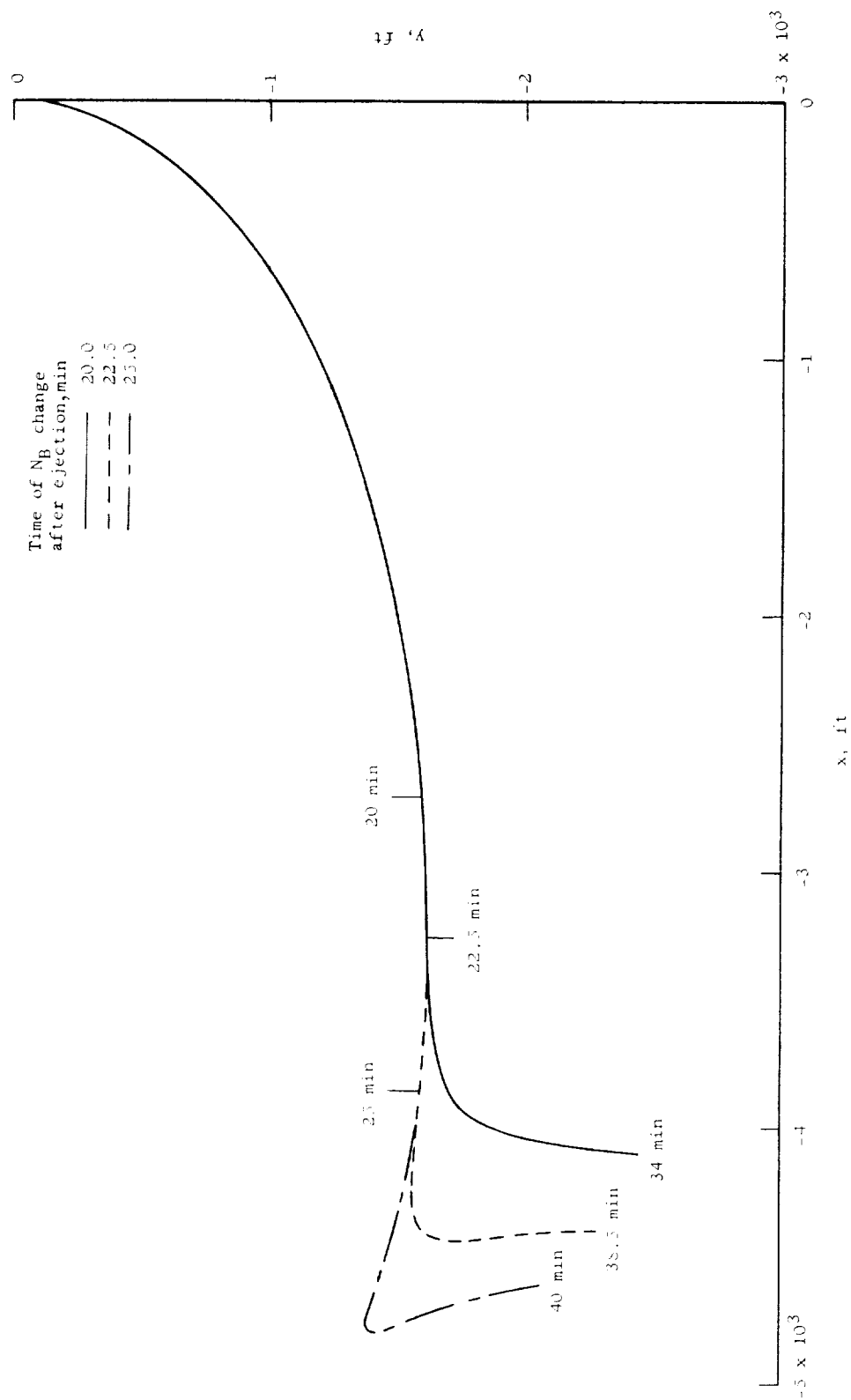
(a) Relative position.

Figure 3.- Position and velocity of the ejected payload relative to the orbiting vehicle. $N_B = 4.5$; 5-minute tick marks.



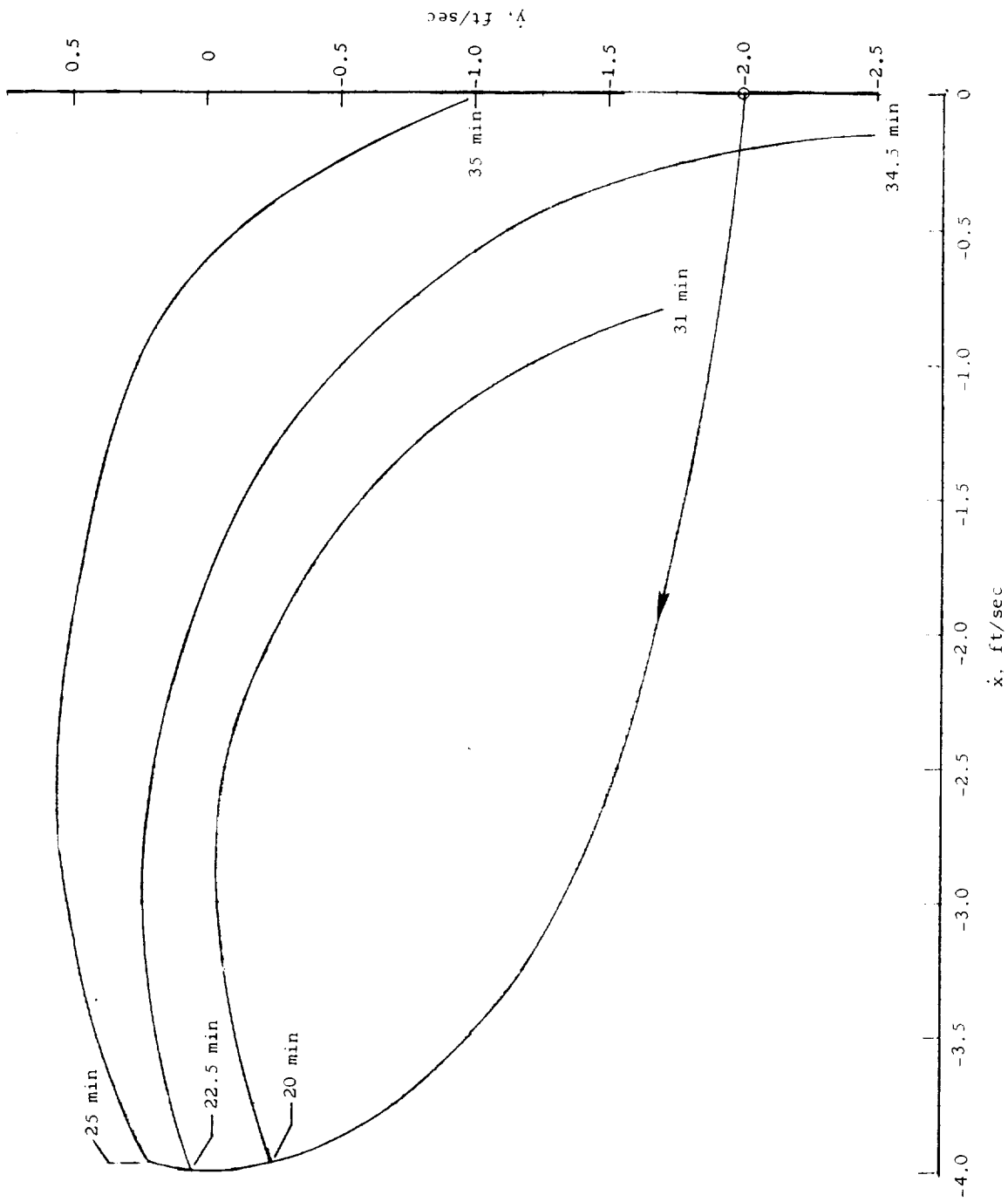
(b) Relative velocity.

Figure 3.- Concluded.



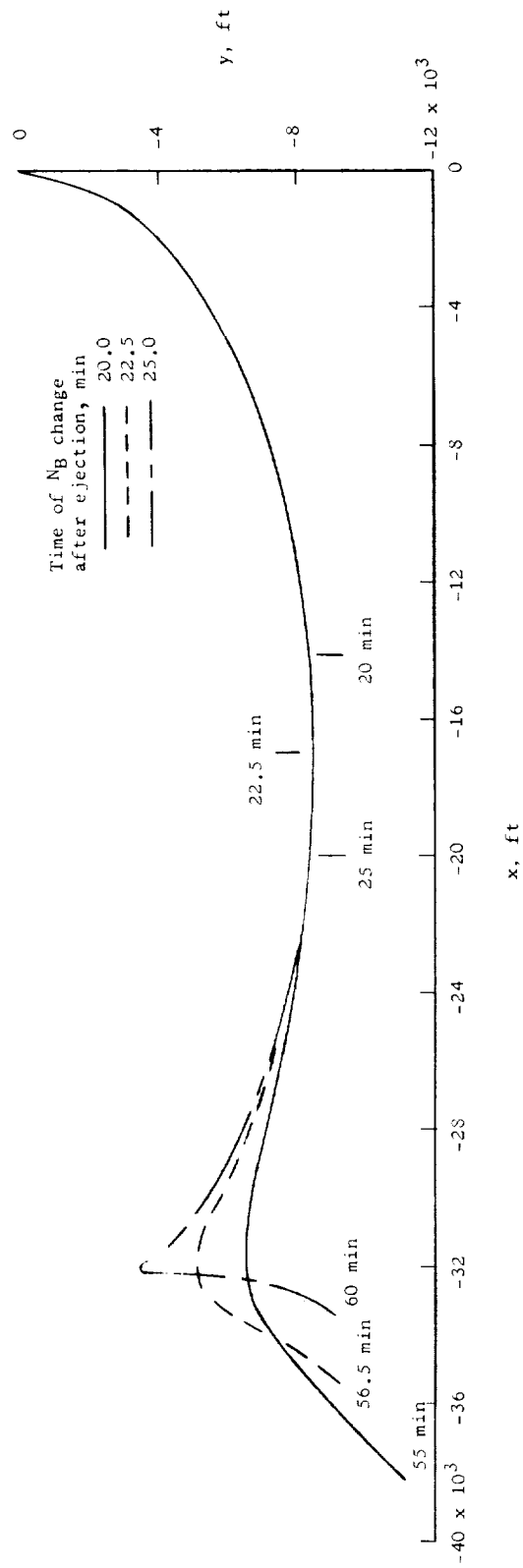
(a) Relative position.

Figure 4.- Relative position and velocity of ejected payload for N_B change from 45 to 0.4 near perigee of the payload orbit. $\dot{x}_0 = 0; \dot{y}_0 = -2$ fps.



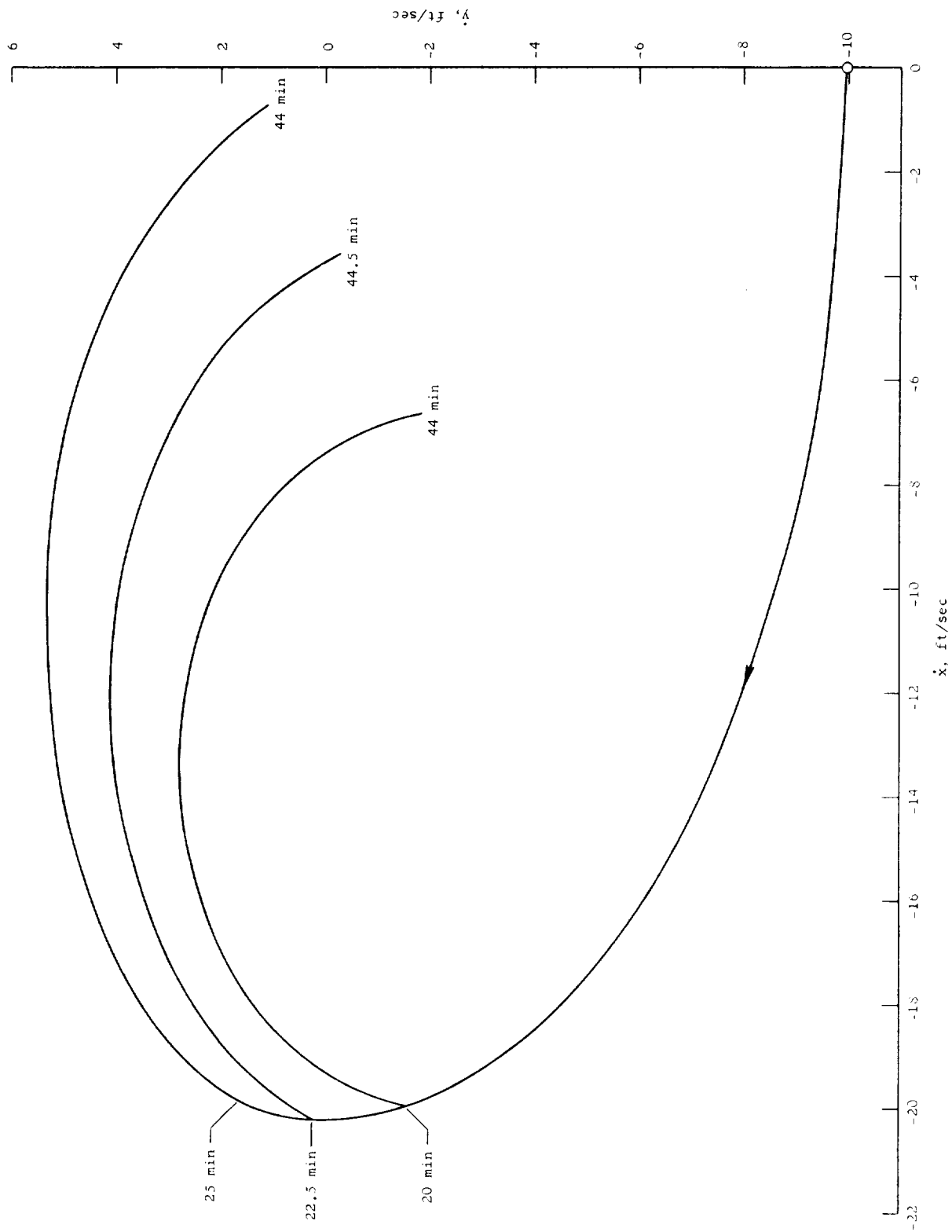
(b) Relative velocity.

Figure 4.- Concluded.



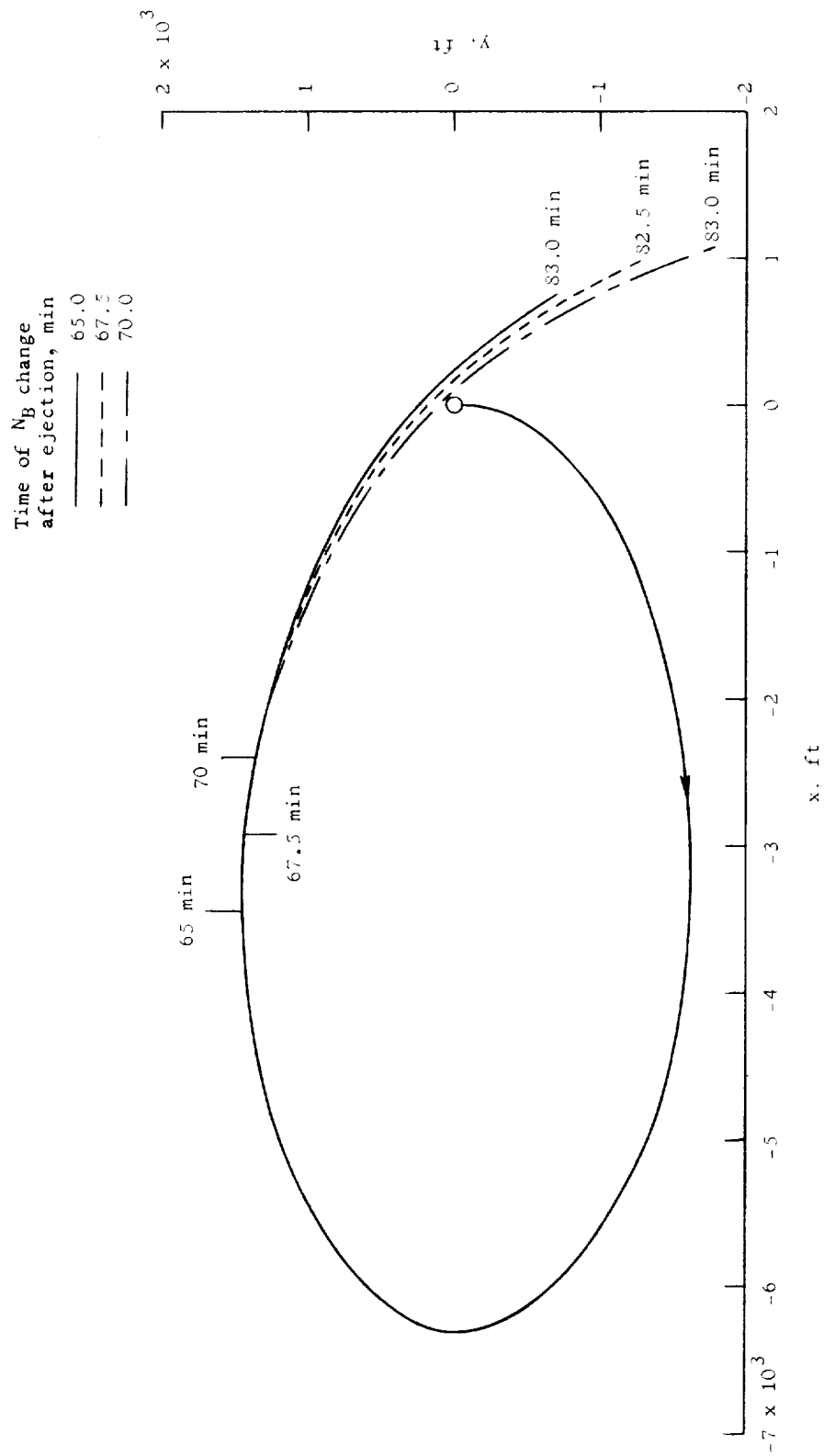
(a) Relative position.

Figure 5.- Relative position and velocity of ejected payload for NB change from 45 to 0.4 near perigee of the payload orbit. $\dot{x}_0 = 0$; $\dot{y}_0 = -10$ fps.



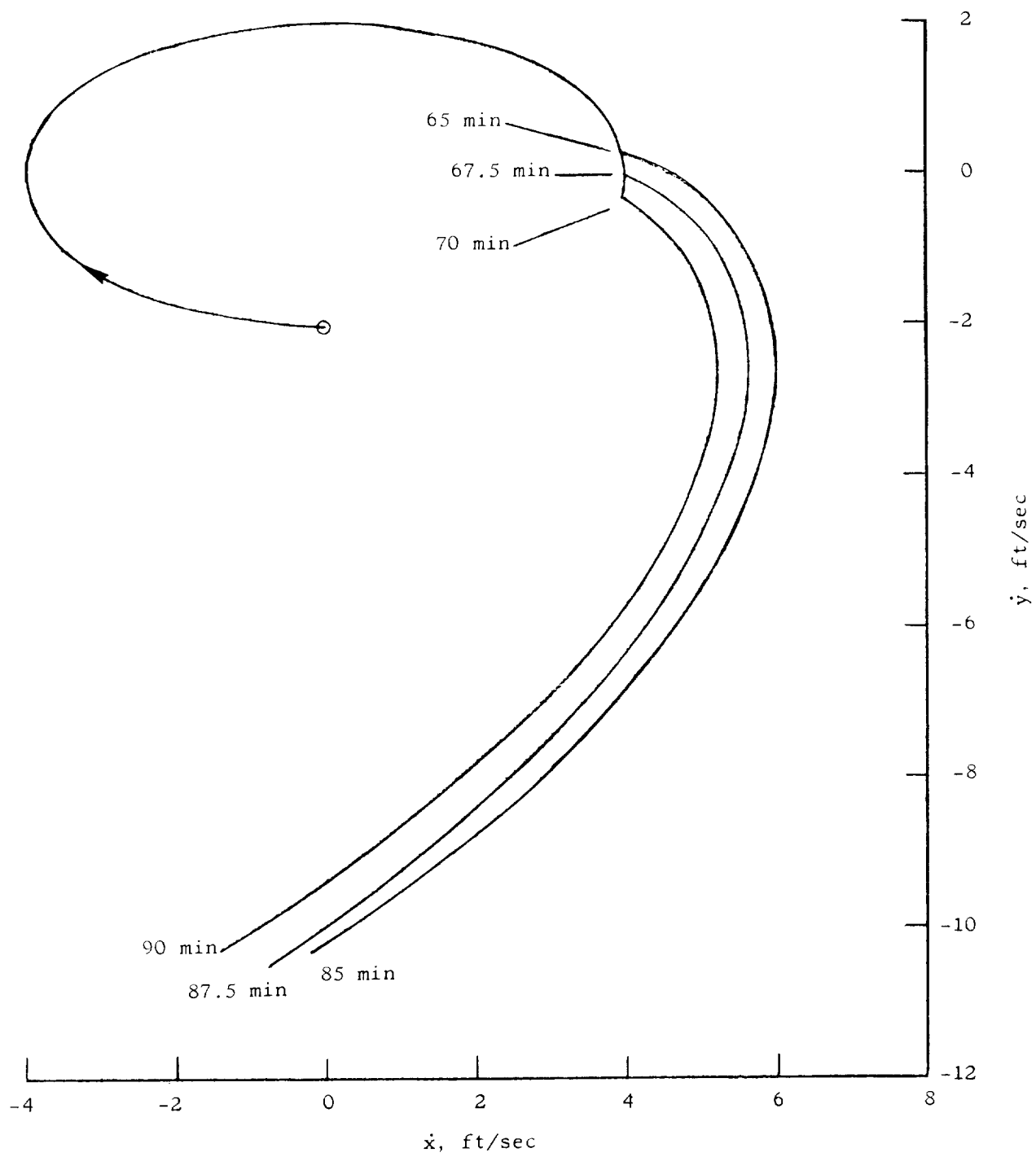
(b) Relative velocity.

Figure 5.- Concluded.



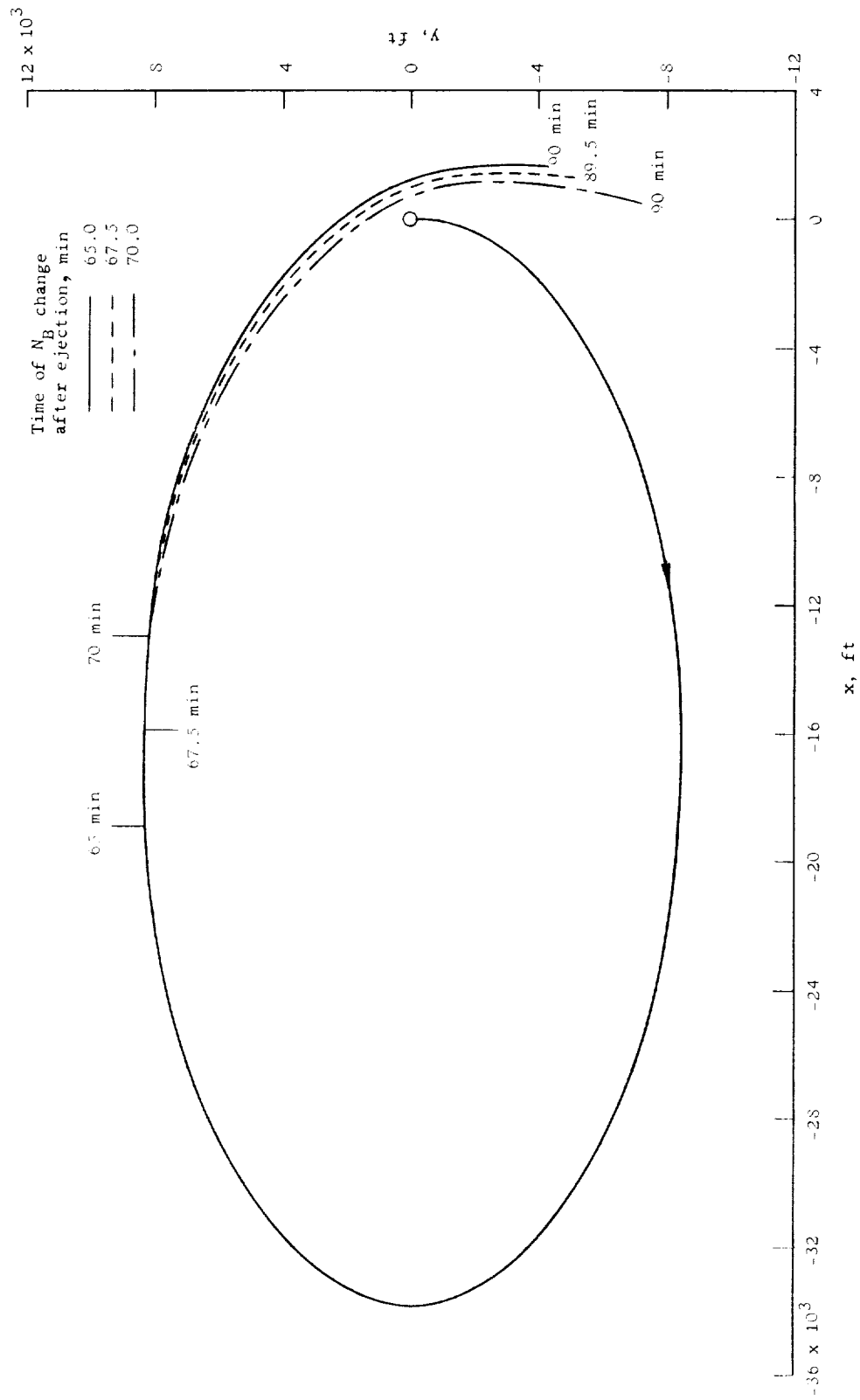
(a) Relative position.

Figure 6.- Relative position and velocity of ejected payload for N_B change from 45 to 0.4 near apogee of the payload orbit. $\dot{x}_0 = 0$; $\dot{y}_0 = -2$ fps.



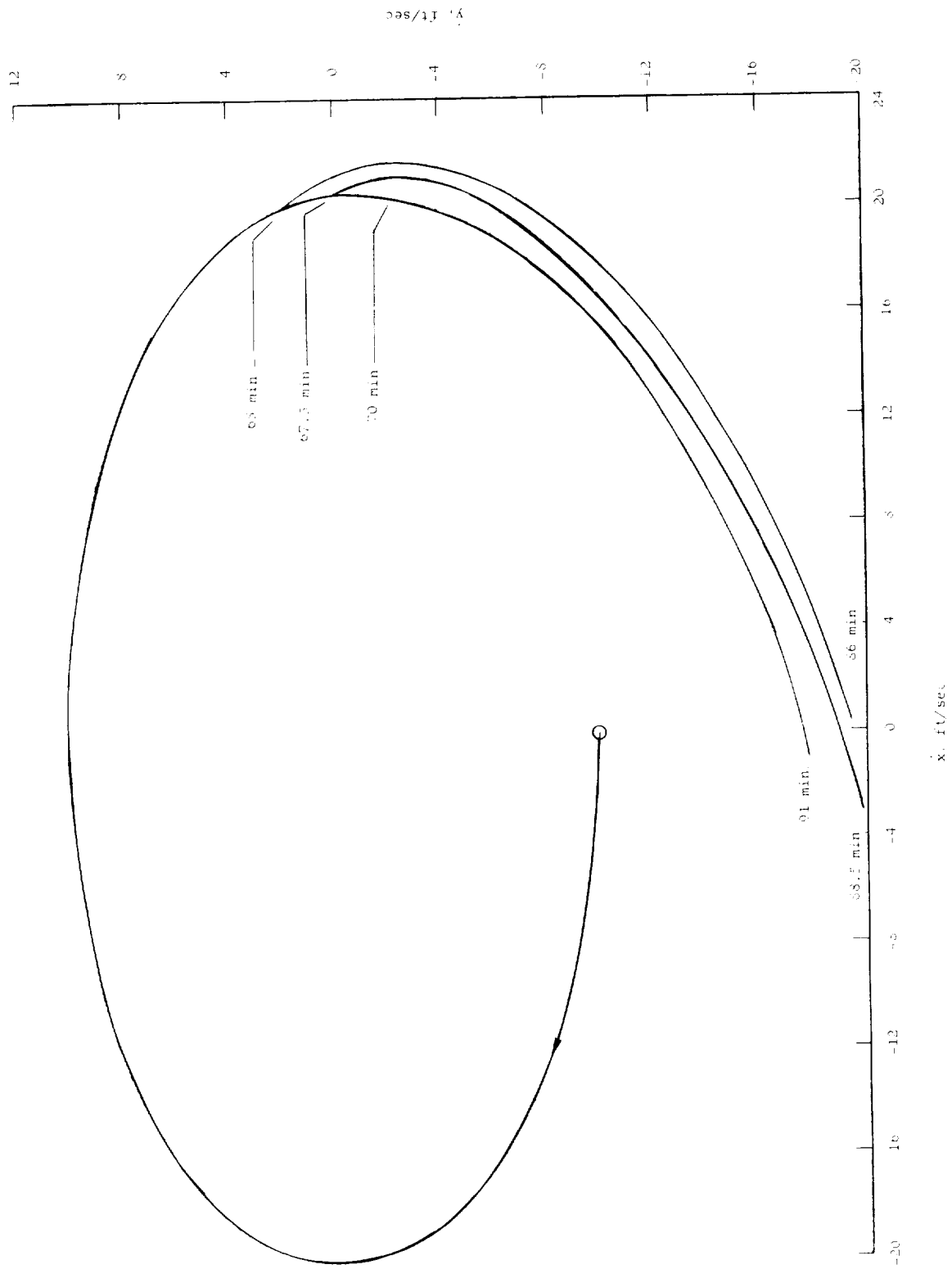
(b) Relative velocity.

Figure 6.- Concluded.



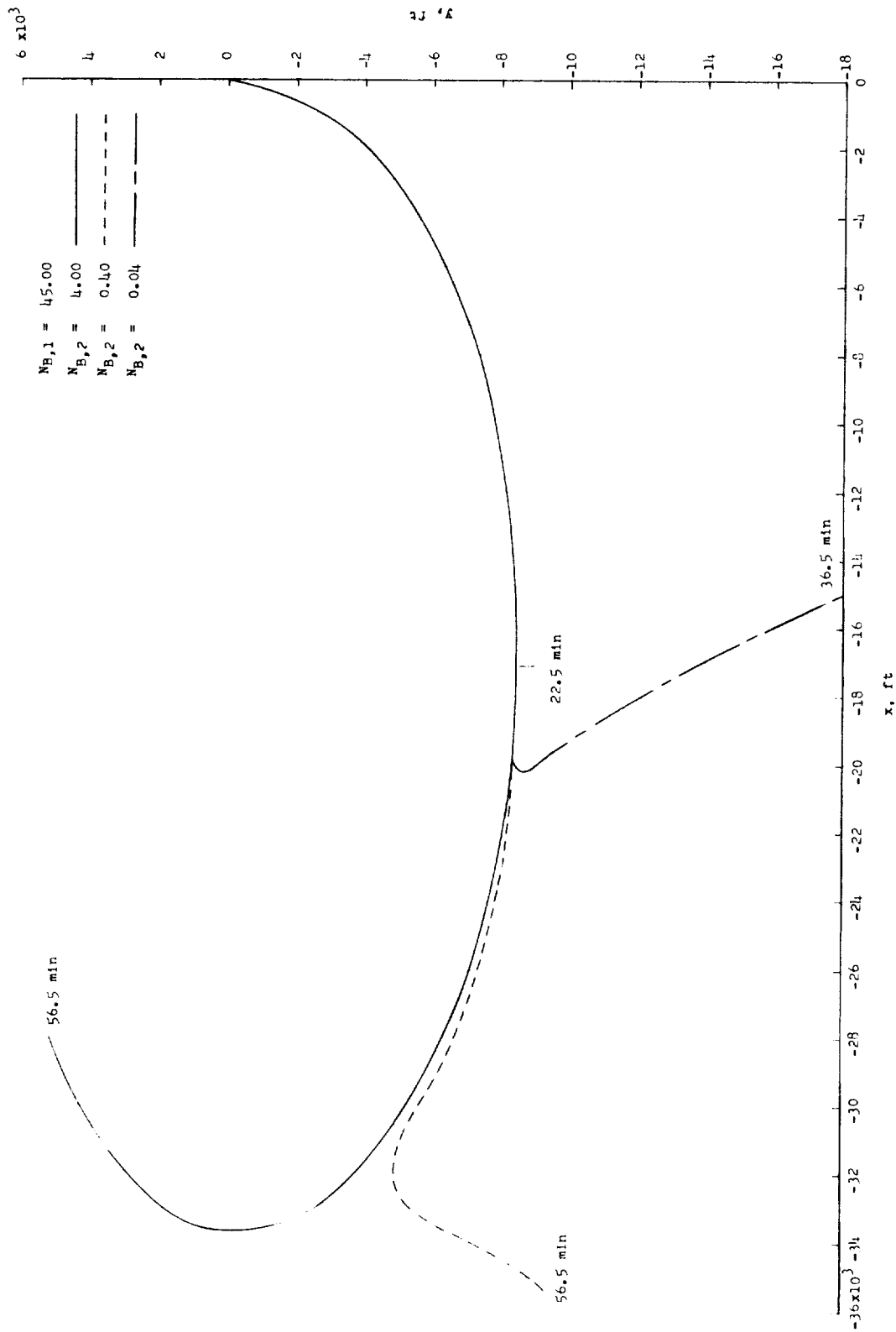
(a) Relative position.

Figure 7.- Relative position and velocity of ejected payload for N_B change from 45 to 0.4 near apogee of the payload orbit. $\dot{x}_0 = 0$; $\dot{y}_0 = -10$ fps.



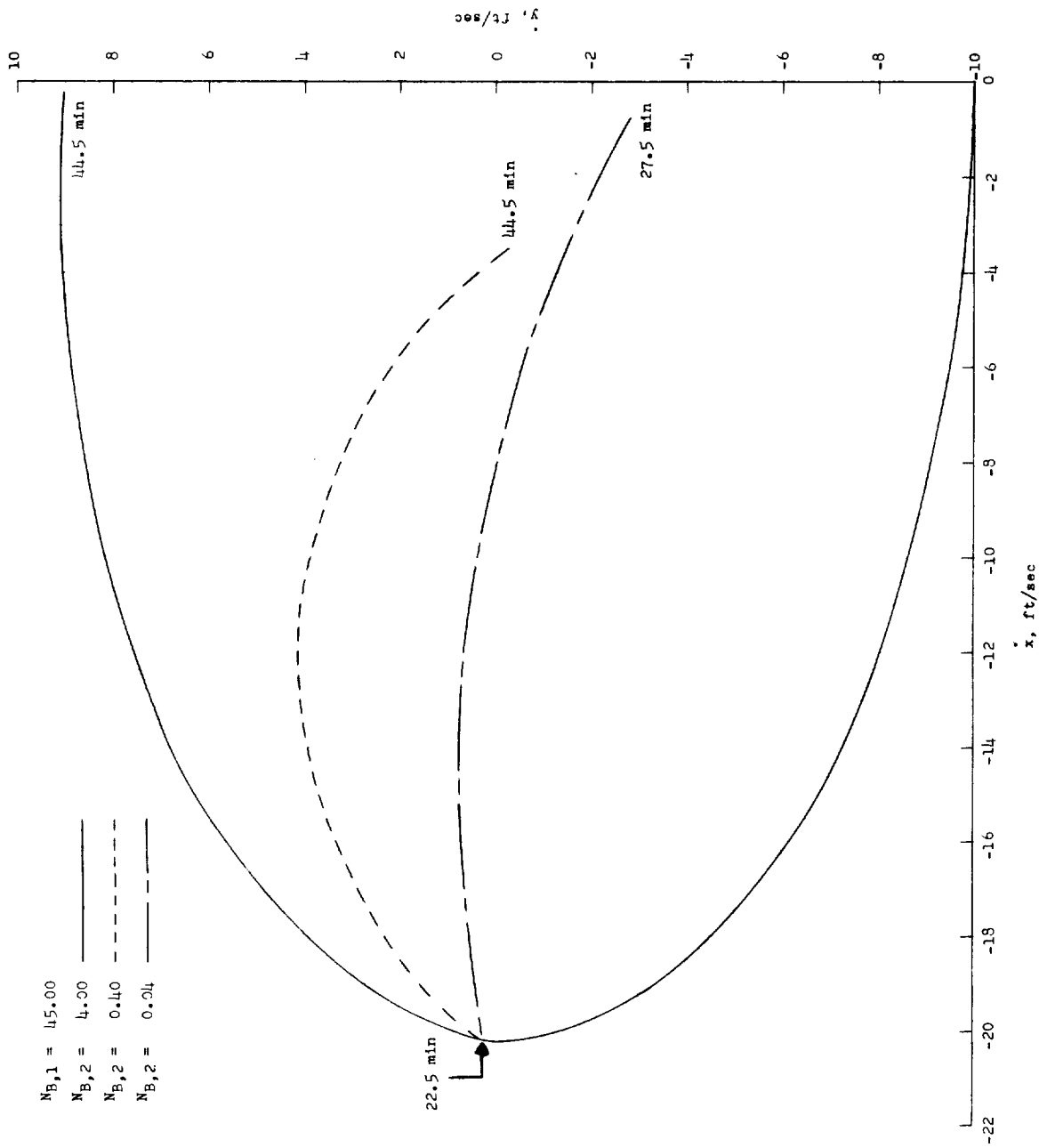
(b) Relative velocity.

Figure 7.- Concluded.



(a) Relative position.

Figure 8.- Relative position and velocity of ejected payload for N_B change from 45 to several different values near perigee of the payload orbit. $\dot{x}_0 = 0$; $\dot{y}_0 = -10$ fps.



(b) Relative velocity.

Figure 8.- Concluded.

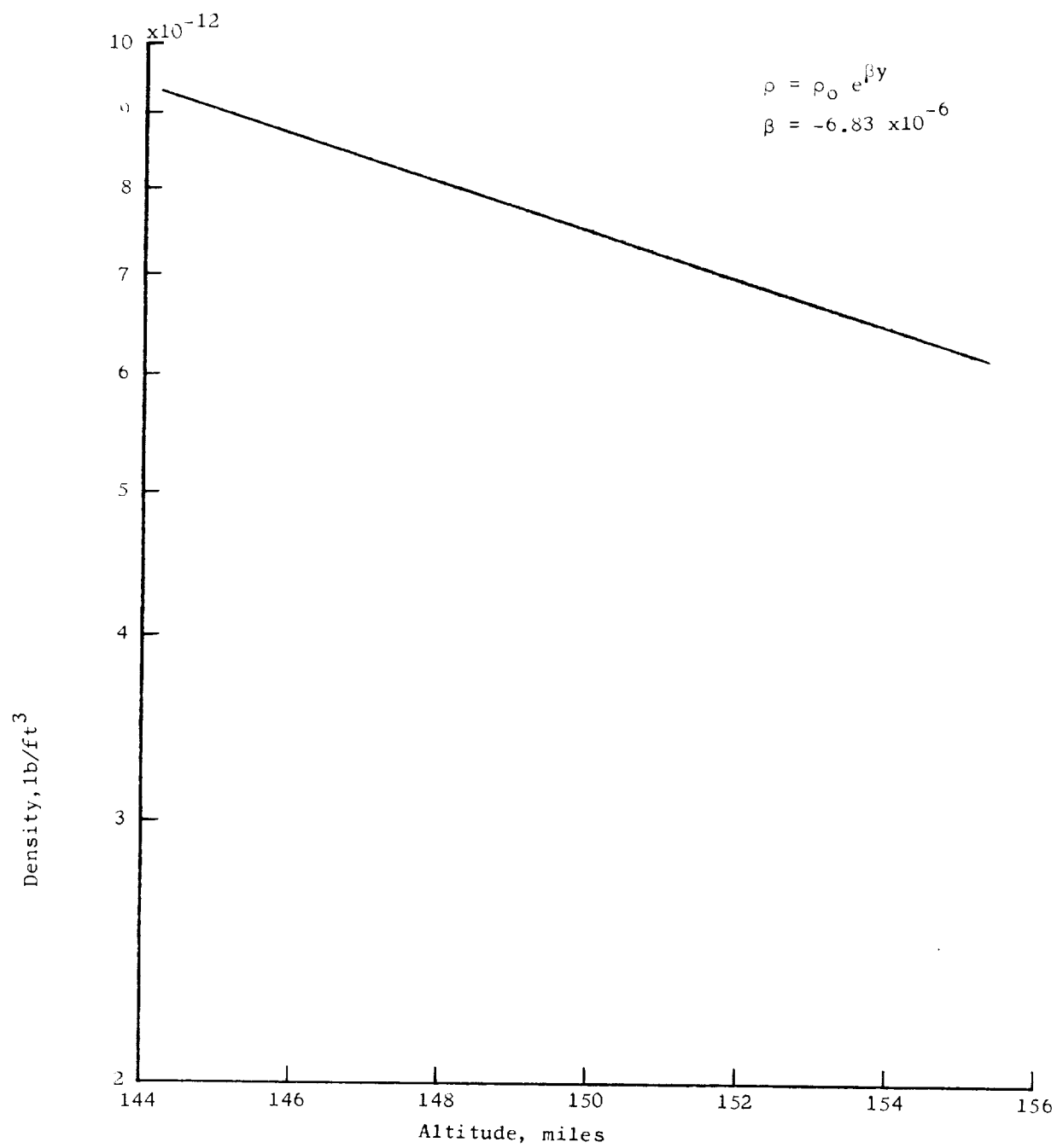


Figure 9.- Weight density of atmosphere as a function of altitude.

1

